Geophysical Journal (1988) **94**, 83–96

Magnetic properties of some synthetic sub-micron magnetites

Barbara A. Maher
School of Environmental Sciences, University of East Anglia, Norwich NR4 7TJ *UK*

Accepted 1987 December 10. Received 1987 December 1; in original form 1987 August 5

SUMMARY
The grain size dependence of various mineral (rock) magnetic parameters has been determined, using a series of essentially pure, fine-grained (single-domain, SD) and ultrafine-grained (superparamagnetic, SP) magnetites. The parameters measured include low-field susceptibility (χ), frequency-dependent $\chi(\chi_{FD})$, saturation remanence (*SIRM*), anhysteretic susceptibility (χ_{ARM}), and coercivity of remanence ($(BO)_{CR}$). The magnetites were produced in experiments designed to simulate possible pedogenic and biogenic pathways of magnetite formation. Their mean grain sizes range from 0.012 μm to 0.06 μm, and hence span the SP/SD boundary. Isothermal magnetic measurements were performed on two separate subsets of differing packing densities. The response of the magnetic parameters is modified by interaction effects, but they display continuous variation across the entire grain size range, confirming their value for rapid magnetic granulometry. Within the fine and ultrafine end of the magnetite grain size spectrum, χ, χ_{FD} and χ_{ARM} are notably responsive to grain size change. In terms of magnetic response (and also possibly of grain size, shape, and absence of cation substitution), these synthetic magnetites represent close analogues of those found in some soils and sediments.

Key words: Magnetic granulometry, mineral magnetism, SP/SD, synthetic magnetites.

INTRODUCTION

Iron oxides are particularly interesting compounds in terms of their geochemical, pedological and magnetic properties. They are environmentally sensitive, often conservative, and, thus, to some extent diagnostic. Innovative application of well-established rock magnetic principles to diverse environmental contexts has produced large amounts of new empirical data, derived from materials ranging from soils and sediments (whether stream, lake, estuarine or deep sea) to snowmelt and atmospheric aerosols (Thompson & Oldfield 1986). The magnetic behaviour of many of these environmental materials appears to be dominated by magnetite or magnetite–maghemite intermediaries. Interpretation of these data, with regard to magnetic mineralogy and grain size, has depended so far on available rock magnetic theory and analogue modelling. Many of the environmental materials, however, display an extremely distinctive type of ferrimagnetic behaviour, as yet poorly modelled by previous rock magnetic work.

Figure 1(a), for example, shows a range of magnetic parameters (and interparametric ratios) obtained for samples from a diver-collected core of Recent sediment from the Potomac River estuary, USA, and Fig. 1(b) shows the same parameters for a soil profile sampled from Exmoor, UK. Each of the data sets exhibits increasing values of low-field susceptibility (χ) and saturation remanence (SIRM), but both are characterized by the occurrence of high values of frequency-dependent χ (χ_{FD})* and anhysteretic remanence (ARM). Further, Fig. 2 illustrates the ARM demagnetization curves for selected samples from the Fig. 1 material: median destructive fields (MDF_{ARM}) are low, and very narrowly between 18 and 22 mT. This pattern of magnetic behaviour, encompassing high frequency-dependence of low-field susceptibility, high χ_{ARM} intensities but of low stability, and concurrent decreases in the $SIRM/\chi_{ARM}$ ratio, has been observed for a number of soil and sediment samples.

A well-defined physical basis exists to account for shifts in the frequency-dependent contribution to low-field susceptibility. Where χ_{FD} (here expressed as a percentage of the low-frequency value) is increased, the presence of ultrafine, superparamagnetic (SP) grains of magnetite is indicated, some of which 'block in' at the higher frequency of measurement (Stephenson 1971). They then no longer contribute as SP but as single-domain (SD) grains; thus, values of high frequency χ can be expected to be proportionally lower than low-frequency values. Until recently, Vincenz's (1965) theoretical calculations also predicted a significant frequency-dependence of susceptibility for multidomain (MD) grains of magnetite. However, as noted by Bloemendal *et al.* (1985), this effect was not observed in measurements on synthetic MD magnetite powders, and a numerical error since detected in the original work accounts for the apparent dualism.

In contrast, the experimental and theoretical grain size dependence of ARM is incompletely known, despite the attention devoted by rock magnetic workers to this parameter, which has been held to be a close room

* χ_{FD} as used here means percentage loss in χ, when measured at high frequency (4.7 kHz), as compared to low frequency (470 Hz).

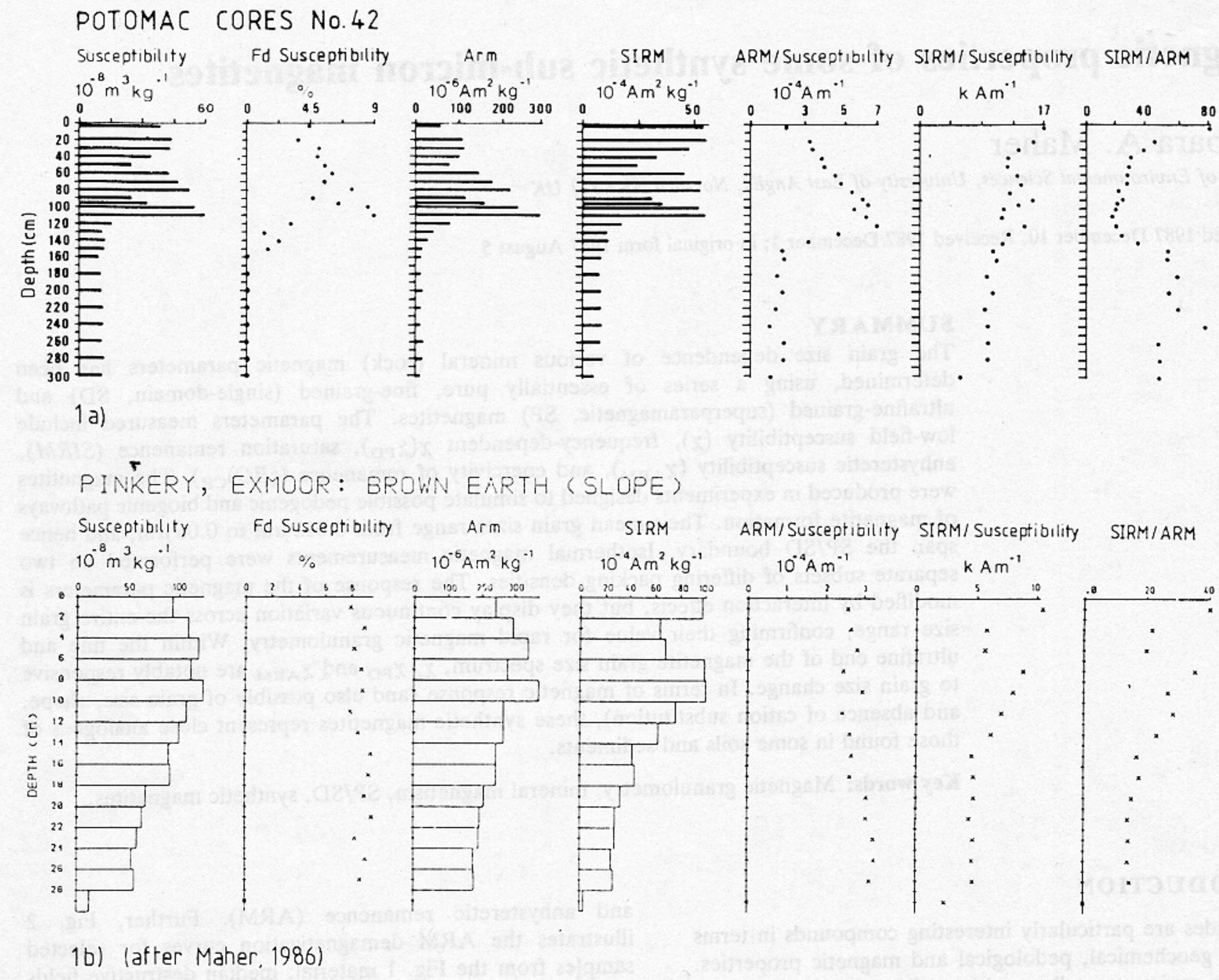

Figure 1. (a) Mineral magnetic data for Core 42, Potomac Estuary. (b) Mineral magnetic data for a brown earth soil profile, Exmoor, UK.

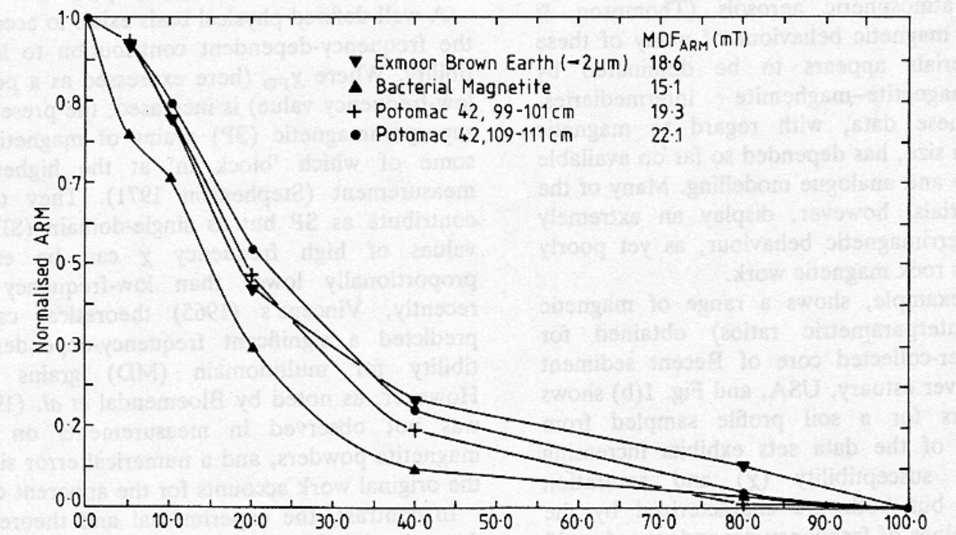

Figure 2. *ARM* demagnetization curves for natural samples.

temperature analogue of thermoremanent magnetization (TRM) (e.g. Levi & Merrill 1976; Johnson *et al.* 1975). Because of the difficulty in obtaining ultrafine-/fine-grained magnetites with controlled, narrow grain size and shape distributions, coupled with an only recent perception of the importance of these grain sizes in rock magnetic contexts (e.g. Morgan & Smith 1981; Petersen *et al.* 1986; Chang & Kirschvink 1985), very few analogues exist for modelling the empirical data. Dankers (1978) suggests that for magnetites and titanomagnetites between '<5 μm' and 150–250 μm both the χ_{ARM} and MDF_{ARM} increase with decreasing grain size. Paradoxical ARM results, comprising high ARM intensities but low stabilities, were reported by Ozdemir & Banerjee (1982) for both natural (soil) and synthetic samples. The latter were synthetic magnetites of controlled sub-micron sizes, of 0.025 μm, 0.12 μm, 0.19 μm and 0.99 μm mean diameters, respectively. The finest sample (somewhat finer than the 0.03 μm SP/SD threshold quoted by Dunlop (1973) for equant magnetite grains) exhibited the highest ARM intensity, and the lowest stability. However, on the basis of these measurements on sized synthetics, and having normalized the ARM data with respect to SIRM, King *et al.* (1983) concluded that 'sub-micron magnetite is very efficient in acquiring ARM and, surprisingly, so is coarse magnetite'. Thus far, then, the granulometric response of ARM at the fine-grained end of the grain size spectrum has been modelled on a very limited number of synthetics.

The present paper reports measurements of χ and various remanences on a newly synthesized series of essentially pure, ultrafine- and fine-grained magnetites, with mean grain sizes ranging from 0.012 to 0.069 μm. The magnetites were produced in experiments designed to simulate possible pathways of magnetite formation in contemporary low-temperature, low-pressure environments (Taylor *et al.* 1987). Slight modifications of the experimental procedure were employed to produce different grain size distributions across the SP/SD boundary. Measurements of isothermal and low-temperature low-field χ, frequency-dependent χ, and of ARM and isothermal remanent magnetization (IRM) acquisition and demagnetization were performed on two separate subsets of this synthetic series in order to (1) determine the dependence of these parameters on magnetite grain size, and (2) provide new analogue data for interpretation of the distinctive ferrimagnetic behaviour displayed by certain soils and sediments, as described above.

SAMPLES AND EXPERIMENTAL PROCEDURES

Synthesis of the magnetite samples was undertaken at the C.S.I.R.O., Division of Soils, S. Australia. The resultant magnetites, and their method of preparation, are described more fully by Taylor *et al.* (op. cit.). From X-ray diffraction, they are essentially pure, although occasional flakes of lepidocrocite are observable under transmission electron microscopy (TEM) (Fig. 3), and consist of single crystals grown from an O_2-purged solution at ambient temperatures and pressures. Grain-size distributions for each sample were determined by digitizing the boundaries of at least 100 grains, outlined on enlarged electron micrographs, with a Houston Complot Series 2000 Digitizer. Table 1 lists the means, ranges and standard deviations of their grain sizes.

All the magnetic measurements were made on 2 cm × . cylindrical samples containing the magnetite dispersed . non-magnetic matrix. The matrix was Analar grade calciu. fluoride, crushed to a fine powder. The degree of dispersion is difficult to control; clustering of the magnetite grains was evident under TEM and can be assumed to occur to some extent within the samples prepared for magnetite analysis. A small known quantity of magnetite of each size of fraction was added to the calcium fluoride and mixed ultrasonically in acetone to form a slurry. The mixing was continued while the acetone evaporated, to maximize grain dispersion. The mixture, once thoroughly dry, was compressed, and immobilized by packing any unoccupied volume of the styrene sample holder with clean cotton wool. The volume of all the prepared samples is $\simeq 10\ cm^3$. Two separate subsets were prepared. In the first (MT) series, the amount of magnetite mixed with the matrix varied between 5 and 100 mg. In the second (New MT) series, packing density was reduced by adding much smaller quantities of magnetite (1–20 mg). Even within both subsets, the packing density can be expected to vary, as a small number of (relatively) coarse grains will weigh the same as a larger number of fine grains.

The magnetic measurements reported here were performed on the prepared dispersions without further modification, i.e. the results obtained are for unannealed grains. This was to avoid possible heat-induced alteration of these extremely fine and already relatively stress-free grains (Dunlop 1986, for example, reported for some sub-micron magnetites a post-annealing decrease in Ms, which he attributed to inversion of a surface layer of γFe_2O_3 to αFe_2O_3).

Room- and low-temperature χ were measured using a dual-frequency (0.47 and 4.7 kHz) Bartington sensor, with a noise level of $\simeq 10^{-9}\ m^3\ kg^{-1}$. The low-temperature measurements were carried out at the Department of Geography, University of Liverpool; the change in χ from liquid nitrogen to room temperature was monitored continuously, and sample temperature recorded using a type-T thermocouple.

All the remaining measurements were carried out at the Geophysics Department, University of Edinburgh. ARMs were imparted in a steady field of 0.1 mT, generated parallel to a superimposed peak AF field of 95 mT, and measured with a Molspin fluxgate magnetometer (noise level $\simeq 10^{-7}\ A\ m^2\ kg^{-1}$).

IRM acquisition behaviour was determined by applying to the initially demagnetized samples a series of incrementally-increasing steady fields, measuring the IRM produced at each step. IRM demagnetization was by single-axis AF rather than DC (backfield) means.

All fields were applied and all remanences measured parallel to the long axis of each sample. An approximately zero-field environment for AF demagnetization was created by enclosing the coil within a triple mu-metal shield.

Additionally, hysteresis properties of the two MT subsets are currently being compiled, and will be reported in a subsequent paper.

Units

SI units are used throughout, as defined in the Appe (which also provides conversion factors to the CGS sys

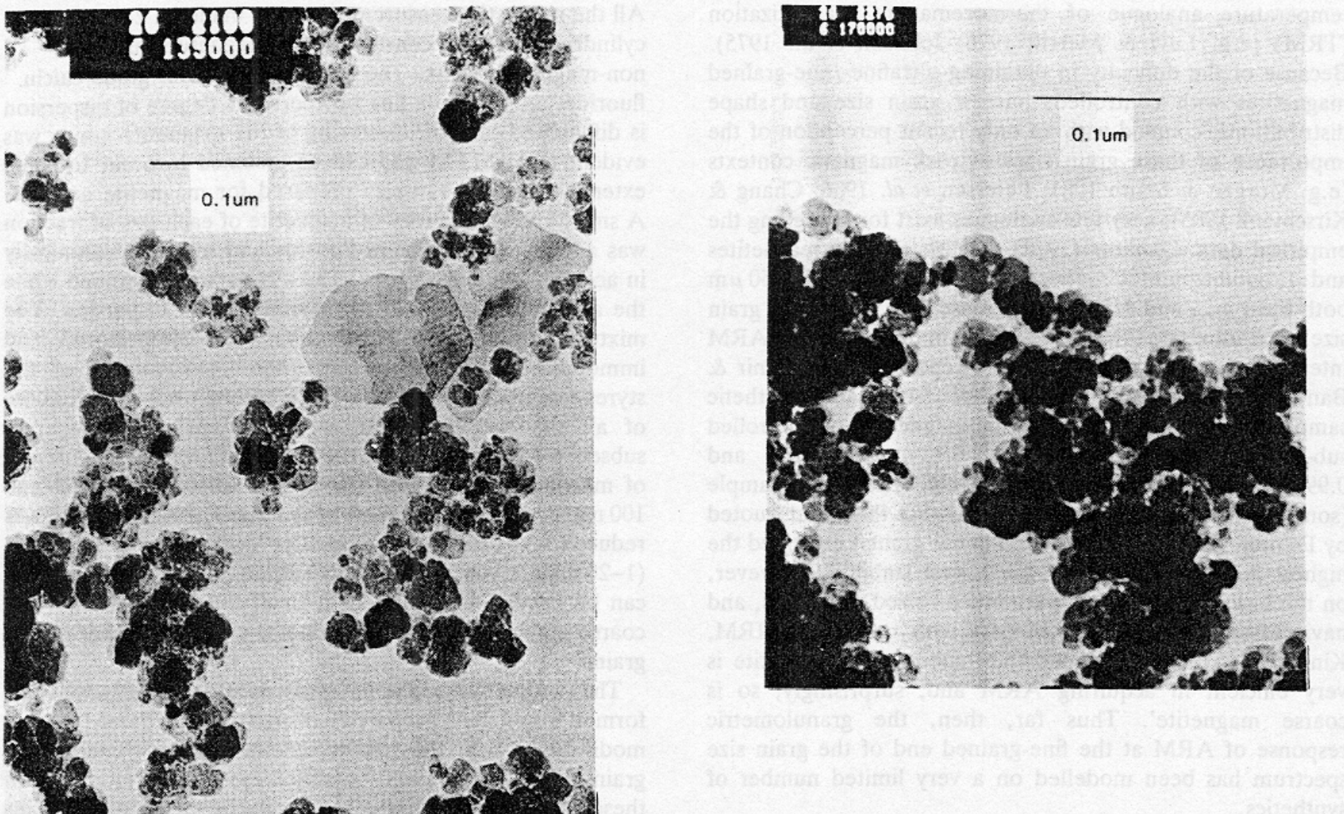

Figure 3. Transmission electron micrographs of MT samples, and associated grain size distributions.

EXPERIMENTAL RESULTS

Room and low-temperature χ, and χ_{FD}

The results of the χ measurements are listed in Table 2. The observed room-temperature χ per gram of magnetite ranges between 513 and 1116 $\mu m^3\ kg^{-1}$, in the studied grain size range of 0.012–0.069 μm. Within this grain size range, there is a marked, exponential increase in χ with decreasing grain size, as can be seen from Fig. 4. For comparison, Fig. 4 also shows published χ data for other dispersed magnetites of controlled grain sizes. Clear trends of χ response are apparent through the entire grain size range, 0.01–500 μm. Dunlop's (1986) observation of a gradual increase in χ with increasing grain size in the sub-micron range is clearly inapplicable here. For grains decreasing in size from 0.036 to 0.01 μm, χ rises from $\simeq$550 $\mu m^3\ kg^{-1}$ to values exceeding 1000 $\mu m^3\ kg^{-1}$. From these SP-dominated χ maxima, values obtained for the grain size range 0.036–0.99 μm then fall from $\simeq$550 to 336 $\mu m^3\ kg^{-1}$, reaching a minimum for the 0.99 μm size fraction. For coarser magnetite grain sizes,

Table 1. MT series: grain size distributions.

Sample I.D.	Mean d (μm)	Range	sd
MT 2	0.02	0.002–0.05	0.011
MT 3	0.015	0.002–0.03	0.007
MT 4	0.014	0.006–0.028	0.005
MT 5	0.012	0.004–0.022	0.003
MT 7	0.012	0.005–0.022	0.003
MT 8	0.017	0.006–0.05	0.006
MT 14	0.022	0.003–0.05	0.009
MT 15	0.023	0.007–0.036	0.007
MT 16	0.02	0.008–0.04	0.008
MT 18	0.016	0.004–0.037	0.005
MT 22	0.034	0.010–0.066	0.013
MT 24	0.031	0.011–0.062	0.012
MT 26	0.036	0.011–0.07	0.014
MT 28	0.032	0.008–0.066	0.012
MT 29	0.069	0.014–0.171	0.03

between 1 and 50 μm, the data of Dankers (1978) shows a significant increase in χ, reaching a secondary, lower peak (relative to the sub-micron fraction) of 716 μm kg χ, at 50 μm. For grains coarser than 50 μm, a gradual decrease in χ is observable. Thus, a continuous trend in χ is displayed from sub-micron to coarse grain-size ranges, despite contrasting modes of grain preparation and sizing: e.g. grown crystals (this paper; Ozdemir & Banerjee 1982) compared with crushed and sieved grains (Dankers 1978).

Definition of magnetic grain size boundaries from the experimental data might place the SP/SD threshold at $\simeq$0.035 μm (very close to Dunlop's (1973) theoretical value), and the PSD/MD boundary at 10–20 μm. A χ minimum would theoretically be predicted for the SD/small PSD size range; the experimental minimum occurs at 0.99 μm, perhaps indicating some shape control in this synthetic sample.

In addition to a grain size dependence, Dankers (1978) noted for χ a packing density effect, χ increasing slightly with a decrease in packing density. Fig. 4 includes the χ data obtained for the second subset of the MT series, in which packing density is much reduced. No clear relationship is apparent between packing density reduction and resulting χ values; there is close replication of the general trend observed for the first MT subset.

Selected samples from the ultrafine- and fine-grained ends of the MT series were subjected to low-temperature χ measurement. SP grains can be expected to produce the most significant changes in χ with temperature; as the temperature is decreased, it passes through the blocking temperatures of the increasingly smaller SP grains, extending their relaxation times beyond the period of χ measurement. Fig. 5 illustrates the changes in χ with temperature for samples MT 26–29 (0.032–0.069 μm) and MT 3 and 7 (0.012–0.015 μm). The χ of the latter group falls by $\simeq$30 per cent from room to liquid-nitrogen temperature. The slightly coarser magnetites, >0.036 μm, display only 13–15 per cent reduction in χ.

Compared with low-temperature analyses, measurements of χ_{FD} can provide an alternative, less time-consuming method of identifying the presence of SP grains employing a higher frequency of AF field (rather than a decrease in measuring temperature) to block in some proportion of the ultrafine fraction. Table 2 lists the percentage values of χ_{FD} obtained for the two separate subsets of the present series. Despite the low-temperature evidence of SP behaviour in the <0.015 μm grain sizes, χ_{FD} percentage values are surprisingly low throughout the entire first subset, ranging from only 0.5–2.9 per cent. (Natural soil samples for comparison, have produced χ_{FD} percentage values of >10 per cent.) In contrast, values for the second subset vary between 0.4 and 11 per cent, with maximum values occurring for the 0.016–0.023 μm size fractions, and minima for the 0.012 and 0.069 μm fractions. Thus, χ_{FD} does *not* show for the first subset the SP contribution demonstrated by the low-temperature measurements. It is possible that those SP grains that would be predicted to block in at the higher frequency used are ineffectively dispersed and are acting as clumped, SD-like grains. This would suggest that the Bartington dual frequency sensor used here, with pre-set frequency levels of 0.47 and 4.7 kHz, detects the response of a very specific, narrow proportion of the SP spectrum, compared to the more comprehensive sensitivity of the low-temperature procedure. In the new MT samples (second subset), grain dispersion is enhanced, and packing density reduced. χ_{FD} values reach a clear peak in the 0.016–0.023 μm fractions. For grains smaller than this, the higher-frequency field is possibly not high enough to block in such fine grains. For grains coarser than $\simeq$0.03 μm, χ_{FD} falls rapidly. The χ of these grains appears dominated by non-viscous, SD behaviour. Mullins (1977) suggested as an upper limit an 8 per cent decrease in χ with a 10-fold increase in frequency. The present data, combined with those of some of the natural (soil and sediment) samples, suggest this is a conservative figure.

Saturation remanence, coercivities of remanence and AF demagnetization

For the first MT subset, the intensities of SIRM range from 0.4–12.5 A m^2 kg^{-1} (as listed in Table 2), and display a marked grain size dependence. The trend is opposite to that shown by χ. SIRM demonstrates a sharp peak in the 0.031–0.036 μm size range, and then decreases at a rapid rate with decreasing grain size, to a minimum in the 0.012 μm fractions (Fig. 6). IRM acquisition curves show that all MT samples attain saturation at fields of between 70 and 300 mT (Fig. 7), the lower saturation fields (70–80 mT) required for the finest fractions, of <0.023 μm, and the higher (100–300 mT) for the >0.31 μm grains. SIRM and IRM acquisition data from the second MT subset closely parallel those of the first set, with the exception that lower peak SIRM intensities were recorded (10.9 A m^2 kg^{-1} compared to 12.5 A m^2 kg^{-1}).

Figure 6 also compares the MT data with other published values for sized magnetite samples. Unlike the progressive pattern of variation shown by χ across the grain size spectrum, two discrete 'spikes' in SIRM intensity appear: one at the 0.03–0.036 μm (SD) grain size range (MT series); the other at the '<5'–10 μm range, as represented by the crushed and sieved natural crystals of Dankers (1978) and Hartstra (1982). However, Parry's (1965) data, for grain sizes within the 1–10 μm range, show only a gradual rise to a very much lower peak in SIRM, occurring at the $\simeq$2 μm grain size. The magnetic properties of the finest crushed natural samples are likely to be affected by grain shape

Table 2. Measured magnetic properties of the MT and New MT samples.

Sample I.D.	Grain size ($\bar{x}$, μm)	Fe_3O_4 by wt (per cent)	χ_{LF} ($\mu m^3\ kg^{-1}$)	χ_{LN2}/χ_{rt}	χ_{FD} (per cent)	*SIRM* ($A\ m^2\ kg^{-1}$)	$(Bo)'_{CR}$ (mT)	MDF_{IRM} (mt)	$(Bo)_{CRint}$ (mT)	'R' ratio	χ_{ARM} ($10^{-5}\ m^3\ kg^{-1}$)	$\chi_{ARM}/\chi_{ARMpredict}$	MDF_{ARM} (mT)
MT 2	0.02	0.48	662		2	4.9	24.5	12	17	0.26	220	0.8	20.5
MT 3	0.015	0.45	809	80	1.6	4.5	21	11	18	0.28	171	0.7	19
MT 4	0.014	0.44	934	70	1.9	1.6	16	8	11	0.27	78	0.6	10
MT 5	0.012	0.32	1000	70	1.2	0.6	15	10	12	0.4	84	1.8	17.5
New MT 5	0.012	0.13	808		0.4	0.3	13.5	9	12	0.37	45	1.6	13
MT 7	0.012	0.07	1055	68	0.5	0.4	11	8	10.5	0.43	80	2.1	14.5
MT 8	0.017	0.36	1116		2.9	0.7	10	5	8	0.34	63	0.7	10
MT 14	0.022	0.89	662		1	6.5	25	11.5	19	0.21	215	0.6	20
New MT 14	0.022	0.17	1034		11	6.2	20	12	16	0.37	1051	2.7	16
MT 15	0.023	0.98	658		0.9	7.6	24	11.5	19	0.24	224	0.6	19
New MT 15	0.023	0.24	798		7	6.3	22	15	19	0.35	798	2.4	17.5
MT 16	0.02	0.63	808		1.6	4.6	22.5	15	18	0.35	182	0.7	20
MT 18	0.016	0.31	809		1.5	5.6	19	8.5	13.5	0.23	248	0.9	14
New MT 18	0.016	0.17	984		10	4.7	18	12	15	0.29	863	2.8	15.5
MT 22	0.034	1.05	667		0.8	7.7	21	12	16	0.25	356	0.97	17
New MT 22	0.034	0.28	691		3	5.7	18	10	15	0.31	713	1.9	14
MT 24	0.031	0.56	546		1	11.5	29	14	23	0.23	416	0.8	29
MT 26	0.036	1.36	634	85	0.7	12.5	28	15.5	20	0.22	465	0.7	25
New MT 26	0.036	0.22	754		2.6	9.6	25	12.5	17.5	0.31	994	1.8	18.5
MT 28	0.032	1.52	625	87	0.7	12.0	29.5	11	20	0.2	344	0.6	19.5
New MT 28	0.032	0.28	731		1.8	8.7	25	12	17	0.25	736	1.4	18
MT 29	0.069	1.52	513	87	0.7	11.2	32.5	16	24	0.29	414	0.9	28
New MT 29	0.069	0.21	524		0.5	9.7	28.5	17	22	0.27	719	1.6	21.5

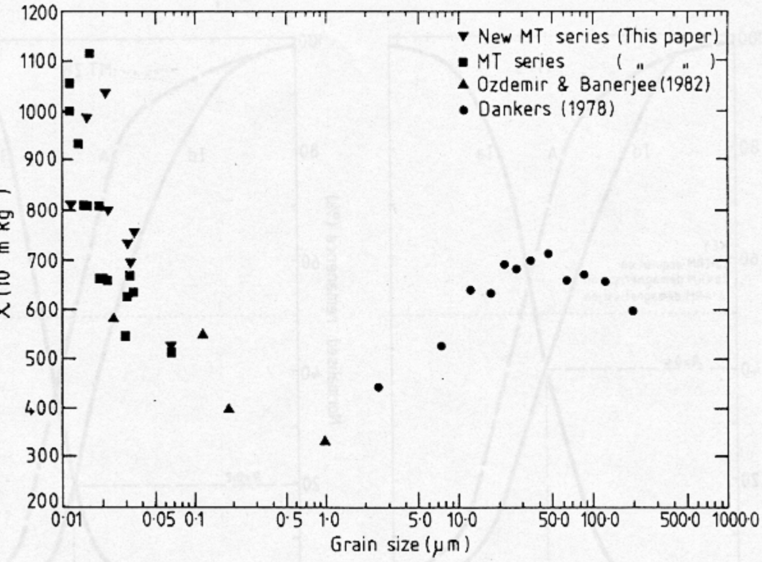

Figure 4. χ vs grain size for MT series and other published data for sized magnetites.

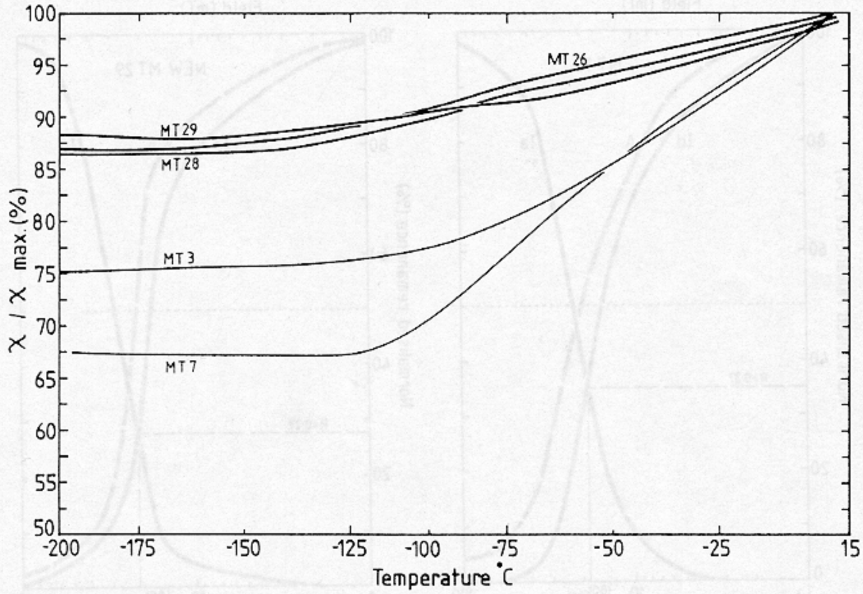

Figure 5. χ vs temperature, MT samples.

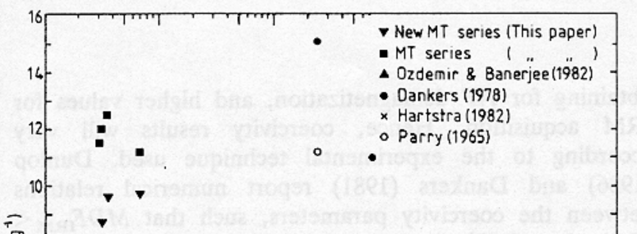

Figure 6. *SIRM* vs. grain size for MT series and other published data for sized magnetites.

irregularities and residual strains induced during sample preparation, and, additionally, by the presence of parasitic finer grains, adhering to the larger particles (see, e.g., Potter & Stephenson 1986). Hence, the apparent peak in SIRM at this coarser end of the spectrum possibly indicates an effectively SD-like grain size, rather than the gross PSD/MD size actually reported for these samples.

At the other end of the grain size spectrum, low (i.e. non-zero) SIRM intensities are indicated even for the ultrafine MT grains (0.012 μm), which would be expected to be incapable of remanence acquisition at room temperature. Small admixtures of SD grains within these samples (Fig. 3) may account for this apparent anomaly; alternatively, interaction between some of the SP grains may be causing collective, SD-like, behaviour, thus expanding the SD range (Morrish & Watt 1957).

Note that Ozdemir & Banerjee (1982) give two data points which span the 0.025–0.12 μm grain size range. Interpolation between these would suggest only a gradual

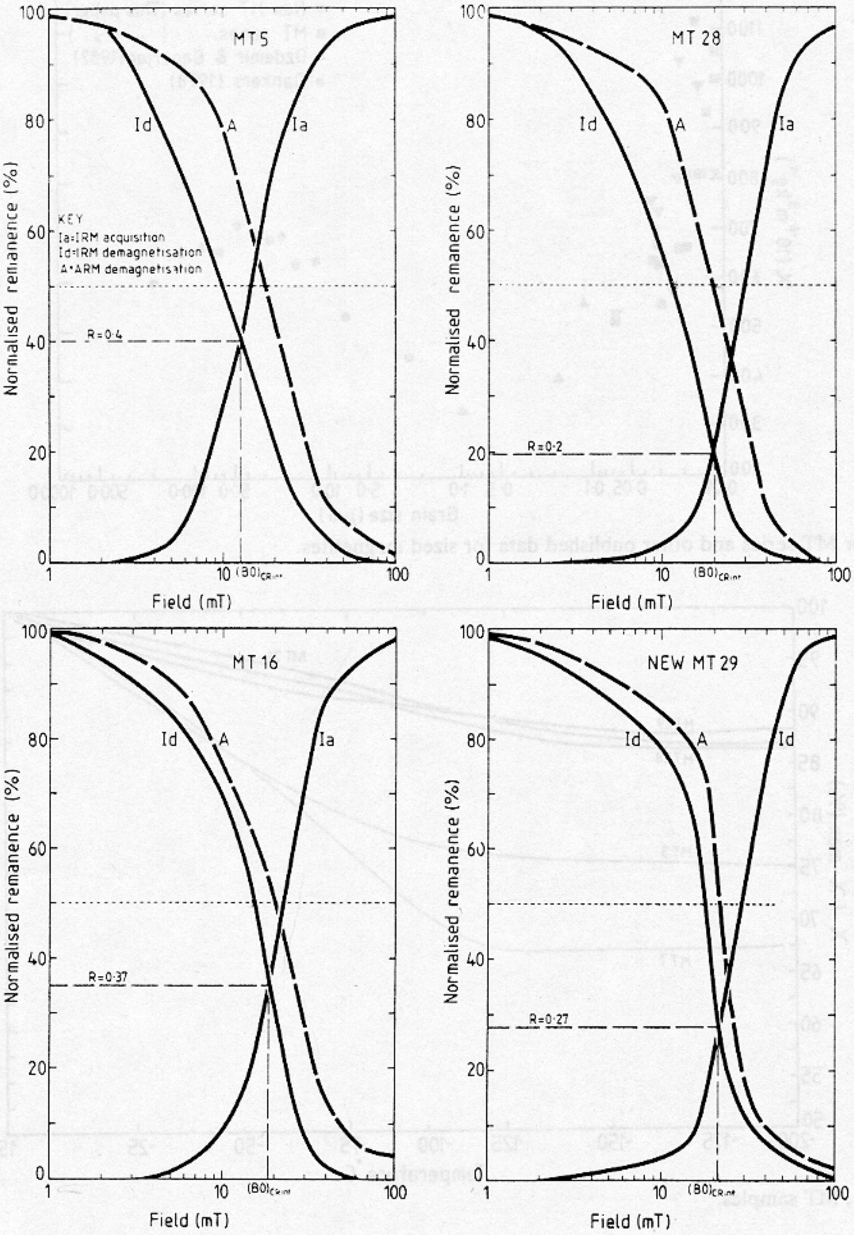

Figure 7. *IRM* acquisition and *AF* demagnetization curves, MT samples.

increase in SIRM with decreasing grain size in this part of the spectrum. The present data, however, indicate a significant peak in SIRM for the size range between these two points.

A variety of coercivity-related parameters are listed in Table 2 for the two MT subsets. The remanent acquisition coercivity ($(BO)'_{CR}$), the median destructive field of IRM (MDF_{IRM}), and the remanent coercivity determined from the intersection of the IRM acquisition and AF demagnetization curves ($(BO)_{CRint}$) are given for each sample. Magnetite has a high magnetic moment and a low coercivity (relative to haematite, for example), and is thus prone to grain interactions and self-demagnetization effects (Dankers 1981). The additional internal fields produced by grain interaction act to oppose creation of IRM and aid in its demagnetization (Dunlop & West 1969). This leads to shifts in the coercivity response, with lower coercivity values obtaining for AF demagnetization, and higher values for IRM acquisition. Hence, coercivity results will vary according to the experimental technique used. Dunlop (1986) and Dankers (1981) report numerical relations between the coercivity parameters, such that $MDF_{IRM} < (BO)_{CR} < (BO)'_{CR}$. Cisowski (1981) shows that the intersection point of the IRM acquisition and demagnetization curves, projected onto the x-axis ($(BO)_{CRint}$), approximates the remanent coercivity ($(BO)_{CR}$), as here the IRM acquired at this field equals the amount of SIRM remaining undemagnetized at this field (Fig. 7).

For the present samples, the $(BO)'_{CR}/(BO)_{CRint}$ ratio varies between 1.0 and 1.5 (mean for first subset = 1.3; for second subset = 1.2). These replicate Dunlop's (1986) results for some SD magnetites, and indicate strong interaction fields. Mean values of 1.4 for PSD-sized material (Dunlop 1986) and 1.7 for MD grains in the range

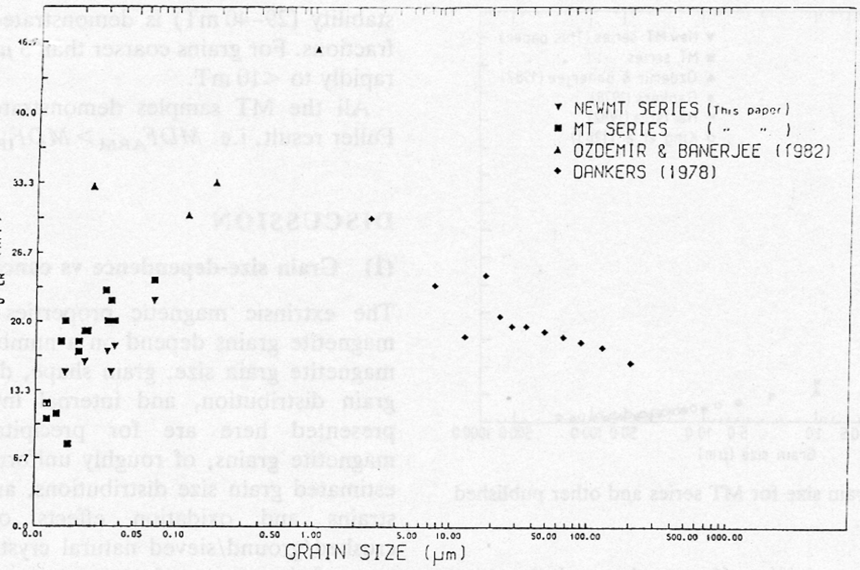

Figure 8. $(BO)_{CR}$ versus grain size for MT series and other published data for sized magnetites.

10–200 μm (Dankers 1981) show that larger grains also display offset acquisition vs demagnetization curves, due to intrinsic internal demagnetizing fields rather than interaction effects. Both the MT subsets conform to the relationship $(BO)'_{CR}+MDF_{IRM}=2(BO)_{CR}$, first reported for coarse magnetite grain sizes by Dankers (1980), and subsequently for fine-grained magnetites by Dunlop (1986).

A further measure of grain interaction, given in Table 2, is Wohlfarth's *R* ratio. This is the ratio of the SIRM, demagnetized to the remanent coercivity field value, to the original SIRM. It is equivalent to the point of intersection of the IRM acquisition and demagnetization curves, projected onto the *y*-axis (Fig. 7). For non-interacting SD magnetite grains, the ratio should be 0.5 (Wohlfarth 1958). For the first MT subset, the ratio varies between 0.2 and 0.43 (mean = 0.28); for the second set it varies between 0.2 and 0.7 (mean = 0.29). This means that a number of the MT samples are more poorly dispersed than are many soil and sediment magnetic assemblages, which are characterized by *R* ratios of ≃0.36. However, the effectiveness of this parameter as a measure of grain dispersion in SP/SD mixtures is open to question. Note the relatively high *R* ratios of MT 16 ($R=0.35$) and MT 8 ($R=0.34$), which span the 0.017–0.02 μm size range. Despite the apparently good dispersion, values of χ_{FD} remain anomalously low (1.6–2.9 per cent). This may indicate clumping of grains in that part of the SP fraction subject to discrimination by this parameter. Conversely, the new MT 14 sample shows an improvement in *R* from 0.21 to 0.37, allied to an increase in χ_{FD} of from 1 to 11 per cent. It seems likely that in this sample, dispersion has been enhanced more evenly across the grain size distribution present.

Figure 8 illustrates the relationship between $(BO)_{CRint}$ and magnetite grain size for the MT subsets, explicitly compared with published $(BO)_{CR}$ values. For the first MT set, values vary from 8 to 24 mT, compared with a range of 12–22 mT for the second set. Within the MT grain size range, coercivities fall linearly from a maximum of 24 mT at 0.069 μm to 8–12 mT at 0.012–0.017 μm. These values seem low compared with Ozdemir & Banerjee's (1982) data, particularly with respect to their 0.025 μm sample, but correspond to some $(BO)_{CR}$ values obtained by Denham *et al.* (1980) for bacterial magnetite grains of 0.04–0.05 μm.

Dunlop (1986) reports for $(BO)_{CR}$ only a weak grain size dependence, and an apparent 'mismatch' between the <1 μm and >1 μm data. His interpretation of a weak negative trend between $(BO)_{CR}$ and grain size in the 0.02–0.2 μm range does not agree with the present data where a roughly linear positive relationship can be observed, from minimum values at 0.012 μm to a peak at 1.0 μm. From 1 to 500 μm, the relationship then inverts to a negative trend, of significantly lower gradient than the positive segment of the data.

As with SIRM, and for similar reasons, low but non-zero $(BO)_{CR}$ values obtain for the ultrafine grained end of the distribution.

Figure 7 shows the IRM AF demagnetization curves for some of the MT samples. All are characterized by slow IRM decay at low and high AF values, and rapid loss at intermediate fields.

χ_{ARM} and AF demagnetization

The dependence of χ_{ARM} (the mass-specific ARM acquired per unit of steady field) on grain size for both MT subsets, and for magnetites from other studies, is illustrated in Fig. 9. For the first MT subset, χ_{ARM} values are minimal ($50–67\times10^{-5}\,m^3\,kg^{-1}$) for the finest, ≃0.012–0.017 μm, grain sizes. They then increase with increasing size, to $171–248\times10^{-5}\,m^3\,kg^{-1}$ in the range ≃0.017–0.023 μm, progressing to a peak, $344–465\times10^{-5}\,m^3\,kg^{-1}$, in the 0.031–0.069 μm size fractions. For the second MT subset, the finest sample, new MT 5 (0.012 μm), confirms the low χ_{ARM} intensity of the ultrafine fractions. From this point on, however, there is a marked divergence between the two data sets. χ_{ARM} values for the new MT samples are up to five times higher than those of the first set, reaching a maximum of $1051\times10^{-5}\,m^3\,kg^{-1}$, and high intensities occur in the 0.016–0.023 μm size range. Table 2 lists for both MT sets the ratios between the experimental χ_{ARM} values and

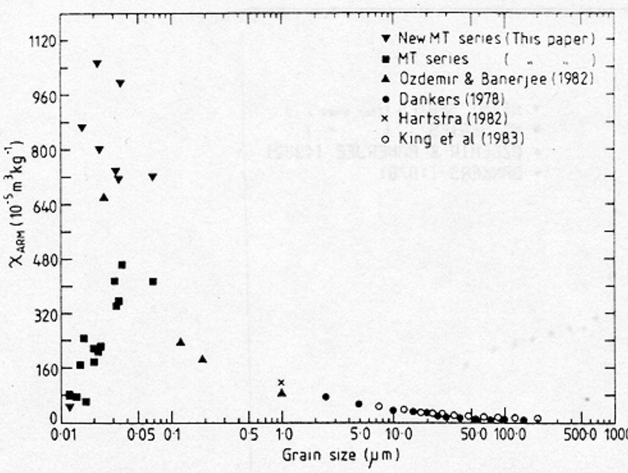

Figure 9. χ_{ARM} versus grain size for MT series and other published data for sized magnetites.

those predicted theoretically (from the relationship, $\chi_{ARM} = SIRM/(BO)_{CR}$; Dankers 1978). For the first set, only MT 5 and MT 7 (both 0.012 μm) have ratios > 1; the remainder vary between 0.6 and 0.97. Without exception, those for the new MT samples exceed unity; new MT 14 (0.022 μm) and MT 15 (0.023 μm) give the highest ratios, 2.7 and 2.8, respectively.

In relation to the other published data, Fig. 9 shows that the two MT data sets lie above and below the 0.025 μm data point of Ozdemir & Banerjee (1982). These researchers' three remaining data points (spanning the 0.12–1 μm size range) then display a slow, continuous decrease in χ_{ARM} with increasing grain size, a pattern which extends right across the coarser end of the grain size spectrum (5–500 μm).

Normalized AF demagnetization of ARM curves was obtained for all MT samples; Table 2 lists the resulting MDF_{ARM} values, and Fig. 10 plots both these and published values against grain size. Ozdemir & Banerjee's (1982) observation of increasing ARM stability with increasing grain size in the sub-micron range is clearly confirmed. Within this range, those grain sizes (0.02–0.36 μm) displaying peak χ_{ARM} values only have low-to-intermediate AF stabilities (10–29 mT; mean = 20 mT). Greatest AF

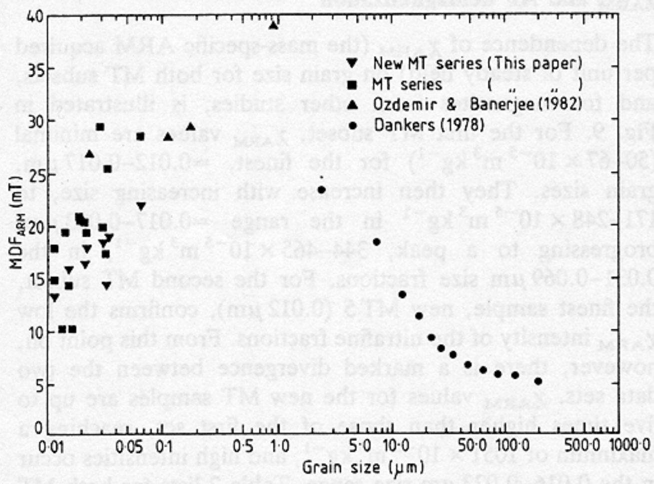

Figure 10. MDF_{ARM} vs. grain size for MT series and other published data for sized magnetites.

stability (29–40 mT) is demonstrated by the 0.1–1 μm size fractions. For grains coarser than 5 μm, MDF_{ARM} values fall rapidly to <10 mT.

All the MT samples demonstrate an SD-type Lowrie–Fuller result, i.e. $MDF_{ARM} > MDF_{IRM}$ (Fig. 7).

DISCUSSION

(1) Grain size-dependence vs concentration dependence

The extrinsic magnetic properties of an assemblage of magnetite grains depend on a number of factors, including magnetite grain size, grain shape, degree of stoichiometry, grain distribution, and internal interactions. The results presented here are for precipitated, essentially pure magnetite grains, of roughly uniform shape, with carefully estimated grain size distributions, and without the residual strains and oxidation effects often associated with crushed/ground/sieved natural crystals. Thus, the dependence of the measured parameters principally on magnetite grain size and on grain distribution (and related grain interaction) can be examined.

Both sets of MT samples show clear variations in parameter response across the studied grain size range of 0.012–0.069 μm, which spans the theoretical SP/SD boundary. Both show an exponential rise in χ with decreasing grain size, a marked peak in SIRM within the 0.031–0.036 μm size range, a $(BO)_{CR}$ maximum in the 0.069 μm fraction, and clearly offset IRM acquisition and demagnetization curves, indicating significant internal fields due to grain interaction. Within the second MT subset, packing density (number of magnetic grains per unit volume of the total specimen) is reduced, and grain dispersion enhanced. Hence, the degree of grain interaction should be reduced overall within the new MT samples. The parameters which appear to be most affected by this change are those of frequency-dependent χ (χ_{FD}) and the intensity of χ_{ARM}. From the anomalously low values (<2 per cent) recorded for the first MT subset, χ_{FD} reaches 7–11 per cent in the new MT samples (peak values occurring in the 0.022 μm size fraction), and the χ_{ARM} intensities of the new MT samples, again in comparison with the original series, reach a greatly increased peak, and occur over a wider grain size range (high intensities being recorded for even the ultrafine, ≃0.02 μm, grain sizes).

These data imply that in the first, less-well-dispersed MT subset grain interactions have caused specific reductions in the populations of those grains that (a) are of SP size but energetically likely to block in between two pre-set frequencies (0.47 and 4.7 kHz) of an applied dc low field; and (b) are most efficient in ARM acquisition. This suggests modification of the reported grain size distribution through clumping of individual grains into larger agglomerates. Not only will this modify the effective grain size distribution (and, hence, parameter response); additional internal fields may be created both between individual grains and between clumps of grains.

The mean $(BO)'_{CR}/(BO)_{CRint}$ ratio of the second MT subset is slightly lower than that of the first series, but still exceeds unity (i.e. the IRM acquisition and demagnetization curves are significantly offset). Thus, interaction effects are still operative within the new MT samples. However, on the basis of the χ_{FD} and χ_{ARM} data, and some of the R ratios (e.g. new MT 14), grain interactions within certain grain size regions appear to be reduced.

The present data may offer at least partial explanation for the apparent paradox of high χ_{ARM} intensities with relatively low stabilities in sub-micron magnetites. The association between these high χ_{ARM} intensities and the theoretically SP-sized fractions (0.017–0.022 μm) suggests clustering of some of the SP grains, resulting in collective SD-like remanence capability (Radhakrishnamurthy *et al.* 1973). Acquisition of weak-field remanences, such as ARM, will be efficient in these clustered grains, the collective size of which will be determined by the number of spins whose interaction energy exceeds thermal agitation. Stability of these clustered SP moments to AF demagnetization will, however, be low, as the moments are not tightly coupled. Such a model would indicate an extension of the otherwise extremely narrow (room temperature) stable SD region in equant-size magnetite (Banerjee & Moskowitz 1985). Within less-well-dispersed samples (e.g. the first MT subset), there may be not only clustering of SP grains to give effectively SD-like moments, but also further interaction between these collective SP/SD grains, and other *bona fide* SD grains. Bridging (two-domain) or other grain configurations may result.

(2) Synthetics as analogues of empirical data

Given that some of the magnetic parameters described here appear to be highly diagnostic of magnetite grain size in these prepared synthetic samples, interpretation of the original empirical data can be attempted using these synthetics as analogue models.

Close correlation between the synthetic and natural data, particularly in terms of χ_{FD} and χ_{ARM} response, occurs in the $\simeq$0.02 μm size range. It is suggested that magnetite grains in this size region ($SP < 0.02\ \mu m > SP/SD, SD$) form a significant component of some natural magnetic assemblages occurring in soils and sediments. This is in contradiction to the observation of King *et al.* (1982) that SP magnetite is not abundant in most natural materials.

Some empirical data derived from environmental contexts remain poorly modelled. For example, χ_{FD} values as high as 20 per cent have been recorded (F. Oldfield, unpub. data), as have even more extreme $\chi_{ARM}/SIRM$ ratios (H. Allen, private communication) than those obtained here for the ultrafine grain size fractions. Totally equivalent magnetic response between synthetic and natural assemblages is likely to be rare, due to a number of factors, including variations in respective grain size distributions, differences in degree of magnetite grain dispersion, and the frequently heterogenous nature of natural assemblages. Although often dominated by magnetite, the magnetic response of natural materials may have various paramagnetic, canted antiferromagnetic, and diamagnetic contributions. Further work is planned to (a) narrow the grain size spread within the synthetic grain size fractions; and (b) assess the magnetic behaviour of mixed synthetic magnetic species.

(3) Rapid granulometric modelling

Identification of grain size variations in magnetite has significance for palaeo-intensity studies, constructing source–sink linkages in environmental systems, and

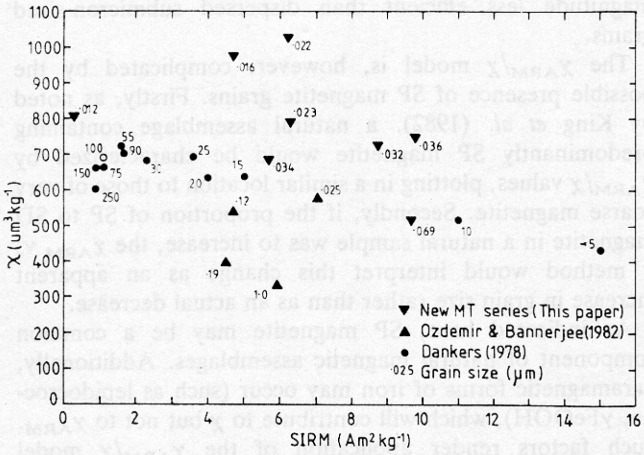

Figure 11. *SIRM*/χ for sized magnetites.

modelling soil iron oxide pathways. For materials in which magnetite is the dominant magnetic species, magnetic methods offer the potential for rapid and non-destructive granulometry, if the grain size dependence of the measured parameters (and/or interparametric ratios) can be shown to be sufficiently size-diagnostic. Thompson & Oldfield (1986) noted that the ratio of *SIRM* to χ can be used as a rough estimate of magnetic grain size. As they further observed, however, mixtures of SP and SD grains give rise to similar *SIRM*/χ ratios as MD grains (Fig. 11). An alternative method of granulometry was proposed by King *et al.* (1982), employing a comparison of χ_{ARM}, rather than *SIRM*, with χ. This method, based on some results for sized magnetites, depends on χ_{ARM} showing particular sensitivity to the SD and small PSD grain sizes, and χ, to the larger PSD and MD grains. Normalizing χ_{ARM} with regard to *SIRM*, these authors reported that sub-micron magnetite was indeed very efficient in acquiring ARM but, surprisingly, so was coarse magnetite. Fig.12 plots normalized χ_{ARM} values ($\chi_{ARM}/SIRM$) against grain size for the MT samples, compared with other published values. (Ozdemir & Banerjee's (1982) data have been recalculated using mass-specific, rather than volume, *SIRM* values). This shows that although MD magnetite is as efficient in ARM acquisition as larger PSD grains, it is nearly an order of

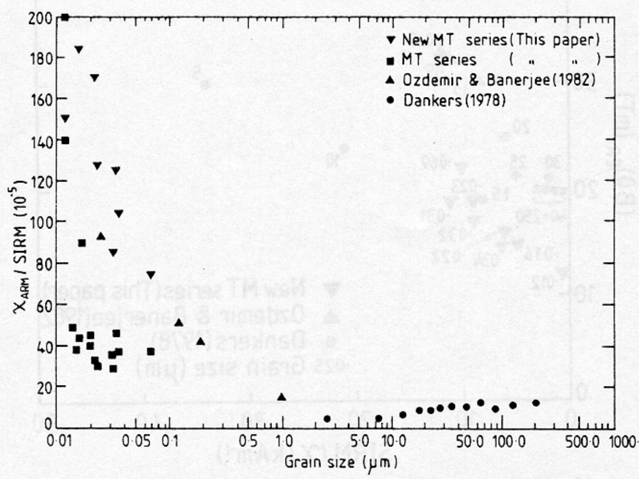

Figure 12. $\chi_{ARM}/SIRM$ vs. grain size for MT series and other published data for sized magnetites.

magnitude less efficient than dispersed submicron-sized grains.

The χ_{ARM}/χ model is, however, complicated by the possible presence of SP magnetite grains. Firstly, as noted by King *et al.* (1982), a natural assemblage containing predominantly SP magnetite would be characterized by χ_{ARM}/χ values, plotting in a similar location to those of very coarse magnetite. Secondly, if the proportion of SP to SD magnetite in a natural sample was to increase, the χ_{ARM} vs χ method would interpret this change as an apparent increase in grain size rather than as an actual decrease.

As indicated here, SP magnetite may be a common component of natural magnetic assemblages. Additionally, paramagnetic forms of iron may occur (such as lepidocrocite, γFeOOH), which will contribute to χ but not to χ_{ARM}. Such factors render application of the χ_{ARM}/χ model problematical. More recently, Bradshaw & Thompson (1985) have advocated use of a $(BO)_{CR}$, $SIRM/\chi$ method of granulometry. They suggest that this combination of parameters would discriminate between SP and coarse MD magnetite assemblages. As indicated in Fig. 13, however, a plot of the prescribed data, derived from sized magnetites, still shows considerable overlap between the two opposite size ranges. A further, practical, disadvantage of this method is that $(BO)_{CR}$ is one of the most time-consuming magnetic parameters to obtain.

In view of these difficulties, a modified, two-stage granulometric method is proposed. The initial stage compares χ_{ARM} not with χ (as in King *et al.*'s (1983) model) but with *SIRM*. This parameter is more size-sensitive *within* the MD range (Fig. 14), and both χ_{ARM} and *SIRM*, as remanence parameters, will be unaffected by paramagnetic contributions. As can be seen from Fig. 14, the only overlap (and, hence, non-discrimination) of grain sizes involves the 0.012 μm and the 150–250 μm magnetites (this paper; Dankers 1978, respectively). Optical microscopy would confirm the presence or absence of the latter grains, as would the proposed second stage of magnetic granulometry. Here, the χ_{ARM} is plotted against either χ_{FD} or the

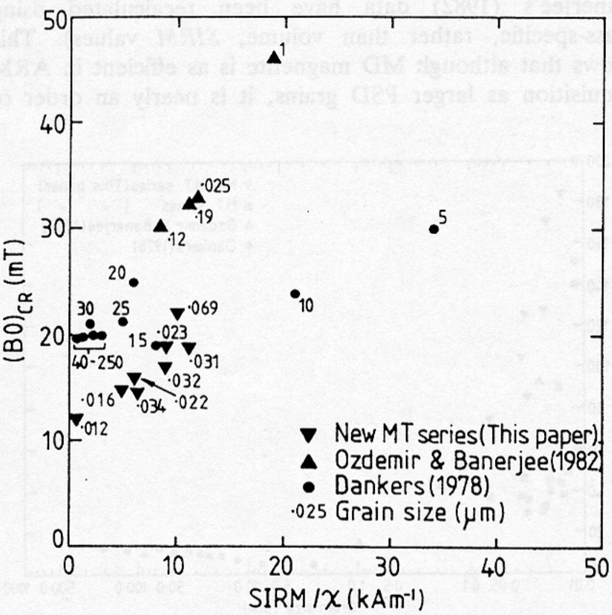

Figure 13. $(BO)_{CR}$ vs. $SIRM/\chi$ for sized magnetites.

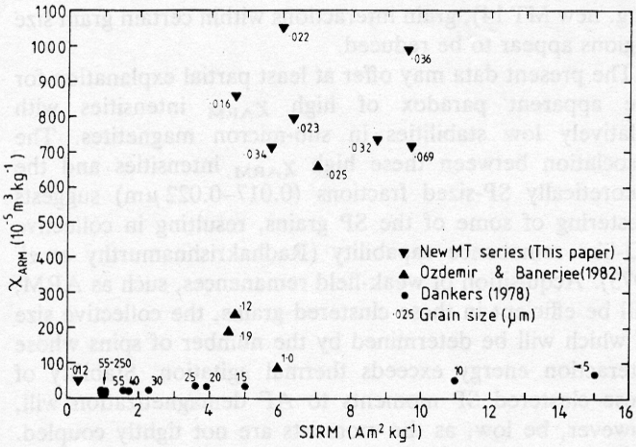

Figure 14. χ_{ARM} vs. *SIRM* for sized magnetites.

MDF_{ARM}, χ_{FD} data is not available for the sized magnetite studies cited here, but Fig. 15 shows the χ_{ARM} vs MDF_{ARM} data. Both of these 'extra' parameters will effectively separate the fine tail from the opposite, coarse end of the grain size spectrum. Fig. 16 shows the sequence of measurements required to implement this method (AF demagnetization of ARM necessarily preceding saturation of remanence).

CONCLUSIONS

1 The MT series of synthetic magnetites, essentially pure and structurally unstrained, provide new analogue data for the grain size range, 0.012–0.069 μm, which spans the theoretical SP/SD boundary. As a result, modelling of parameter response across this ultrafine–fine grained end of the magnetite size spectrum can be greatly improved; previously reported mismatches between the data sets from the sub-micron and the >1 μm sized magnetites appear to be due to dependence on insufficient data points.

2 The observed grain size dependence of the magnetic parameters is significantly affected by the degree of dispersion of the magnetite grains, and, hence the level of interaction between them. The parameters most influenced by interaction effects in the present samples are χ_{FD} and χ_{ARM}. With decreasing packing density, both parameters show marked sensitivity to the $\simeq$0.02 μm grain size range. It is difficult to obtain, in the synthetic

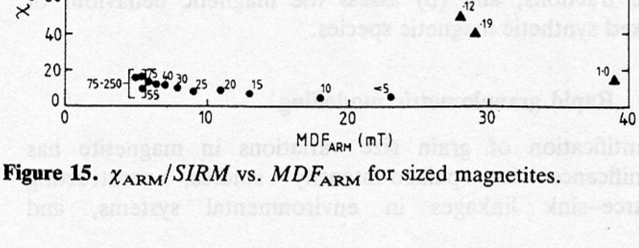

Figure 15. $\chi_{ARM}/SIRM$ vs. MDF_{ARM} for sized magnetites.

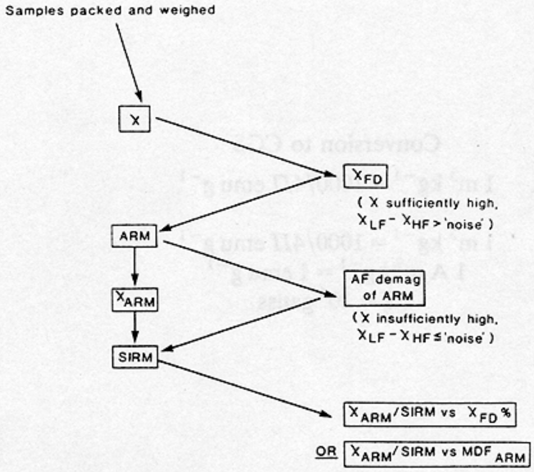

Figure 16. Sequence of measurements required for new granulometric method.

grains, the degree of dispersion shown by natural samples, as measured by Wohlfarth's *R* ratio.

3 Within the grain size range studied, those grains of $\simeq 0.02\,\mu$m (SP, SP/SD) generate magnetic behaviour which closely corresponds to the distinctive pattern recorded for some natural soil and sediment samples. It is suggested that the synthetic grains represent good analogues of the natural ferrimagnetic assemblages. SP and SP/SD magnetite thus appears to be a common component of such assemblages.

4 On the basis of the present data, a new method of magnetic granulometry is proposed. The problem of poor magnetic discrimination between SP- and coarse-MD dominated assemblages may be resolved by comparing the $\chi_{ARM}/SIRM$ ratio with either χ_{FD} or the MDF_{ARM}. The latter two parameters will identify the fine grained tail from the opposite, coarse end of the grain size spectrum.

ACKNOWLEDGMENTS

The author thanks the Nuffield Foundation, and C.S.I.R.O. Soils Division, for financial support for this project, Mr D. Mew for assistance with diagrams, Miss R. Cullington for typing the draft of this paper, and Mr D. Watson, of the Geophysics Department, University of Edinburgh, for taking the time to repair abandoned equipment. This work was carried out during tenure of a Natural Environmental Research Council (UK) Research Fellowship.

REFERENCES

Banerjee, S. K. & Moskowitz, B. M., 1985. Ferrimagnetic properties of magnetite, in *Magnetite Biomineralisation and Magnetoreception in Organisms*, eds Kirschvink, J. L., Jones, D. S. & MacFadden, B. J., Plenum Press, New York & London.

Bloemendal, J., Barton, C. E. & Radhakrishnamurthy, C., 1985. Correlation between Rayleigh loops and frequency-dependent and quadrature susceptibility: application to magnetic granulometry of rocks, *J. geophys. Res.*, **90,** 8789–8792.

Bradshaw, R. & Thompson, R. 1985. The use of magnetic measurements to investigate the mineralogy of Icelandic lake sediments and to study catchment processes, *Boreas,* **14,** 203–215.

Chang, S. R. & Kirschvink, J. L., 1985. Possible biogenic magnetite fossils from the late Miocene Potamida Clays of Crete, in *Magnetite Biomineralisation and Magnetoreception in Organisms,* eds Kirschvink, J. L., Jones, D. S. & MacFadden, B. J., Plenum Press, New York & London.

Cisowski, S. 1981. Interacting vs non-interacting single domain behaviour in natural and synthetic samples, *Phys. Earth planet. Int.*, **26,** 52–56.

Dankers, P. H. 1978. Magnetic properties of dispersed natural iron oxides of known grain size, *PhD thesis,* University of Utrecht.

Dankers, P. H. 1981. Relationship between median destructive field and remanent coercive forces for dispersed natural magnetite, titanomagnetite and hematite, *Geophys. J. R. astr. Soc.,* **64,** 447–461.

Denham, C. R., Blakemore, R. P. and Frankel, R. B. 1980. Bulk magnetic properties of magnetotactic bacteria, *IEEE Trans. Mag.,* **Mag-16,** 1006–1007.

Dunlop, D. J. 1973. Superparamagnetic and single domain threshold sizes in magnetite, *J. geophys. Res.*, **78,** 1780–1793.

Dunlop, D. J. 1986. Hysteresis properties of magnetite and their dependence on particle size: a test of pseudo-single-domain remanence models, *J. geophys. Res.*, **91,** 9569–9584.

Dunlop, D. J. & West, G. F., 1969. An experimental evaluation of single domain theories, *Rev. Geophys. Space Phys.,* **1,** 709–757.

Hartstra, R. L., 1982. Grain-size dependence of initial susceptibility and saturation magnetisation-related parameters of four natural magnetites in the PSD-MD range, *Geophys. J. R. astr. Soc.,* **171,** 477–495.

Johnson, H. P., Lowrie, W. & Kent, D. V., 1975. Stability of anhysteretic remanent magnetisation in fine and coarse magnetite and maghemite particles, *Geophys. J. R. astr. Soc.,* **41,** 1–10.

King, J. W., Banerjee, S. K. & Marvin, J., 1983. A new rock-magnetic approach to selecting sediments for geomagnetic palaeointensity studies: application to palaeointensity for the last 4000 years, *J. geophys. Res.*, **88,** 5911–5921.

Levi, S. & Merrill, R. T., 1976. A comparison of ARM and TRM in magnetite, *Earth planet. Sci. Lett.*, **32,** 171–184.

Maher, B. A., 1986. Characterisation of soils by mineral magnetic measurements, *Phys. earth Planet. int.*, **42,** 76–92.

Morgan, G. E. & Smith, P. P. K., 1981. Transmission electron microscope and rock magnetic investigations of remanence carriers in a Precambrian metadolerite, *Earth planet. Sci. Lett.*, **53,** 226–240.

Morrish, A. H. & Watt, A. R., 1957. Effect of the interaction between magnetic particles on the critical single-domain size, *Phys. Rev.*, **105,** 1476–1478.

Mullins, C. E., 1977. Magnetic susceptibility of the soil and its significance in soil science: a review, *J. Soil Sci.*, **28,** 223–246.

Ozdemir, O. & Banerjee, S. K., 1982. A preliminary magnetic study of soil samples from west-central Minnesota, *Earth planet Sci. Lett.*, **59,** 393–403.

Parry, L. G., 1965. Magnetic properties of dispersed magnetite powders, *Phil. Mag.*, **11,** 303–312.

Petersen, N., von Dobeneck, T. & Vali, H., 1986. Fossil bacterial magnetite in deep-sea sediments from the S. Atlantic ocean, *Nature,* **320,** 611–615.

Potter, D. K. & Stephenson, A., 1986. The detection of fine particles of magnetite using anhysteretic and rotational remanent magnetisation. *Geophys. J. R. astr. Soc.,* **87,** 569–582.

Radhakrishnamurthy, C., Sastry, N. P. & Deutsch, E. R., 1973. Ferro-magnetic behaviour of interacting superparamagnetic particle aggregates in basaltic rocks, *Pramana,* **1,** 61–65.

Stephenson, A., 1971. Single domain grain distributions. 1. A method for the determination of single domain size distributions, *Phys. Earth planet. Int.*, **4,** 353–360.

Taylor, R. M., Maher, B. A. & Self, P. G., 1988. Magnetite in soils. I. The synthesis of superparamagnetic and single domain magnetite. *Clay Minerals,* 1987, **22,** 411–422.

Thompson, R. & Oldfield, F., 1986. *Environmental Magnetism,* Allen & Unwin, London.

Vincenz, S. A., 1965. Frequency dependence of magnetic susceptibility of rocks in weak alternating fields, *J. geophys. Res.*, **70,** 1371–1377.

Wolhfarth, E. P., 1958. Relations between different modes of acquisition of the remanent magnetisation of ferromagnetic particles, *J. Appl. Phys.*, **29,** 595–596.

APPENDIX 1

SI units and conversion factors

	Symbol	SI unit	Conversion to CGS
Mass susceptibility	χ	$m^3\ kg^{-1}$	$1\ m^3\ kg^{-1} = 1000/4\Pi$ emu g^{-1}
Mass anhysteretic susceptibility	χ_{ARM}	$m^3\ kg^{-1}$	$1\ m^3\ kg^{-1} = 1000/4\Pi$ emu g^{-1}
Mass magnetization	e.g. *SIRM*	$A\ m^2\ kg^{-1}$	$1\ A\ m^2\ kg^{-1} = 1$ emu g^{-1}
Magnetic induction	B	T	$1\ T = 10^4$ gauss